A STUDY ON THE PREDICTION OF THE THERMAL ENVIRONMENT IN A LARGE GLASS COVERED ATRIUM USING NATURAL VENTILATION

Kiyoshi Hiwatashi[1], Yasushige Morikawa[1], Keiko Sugawara[1],Yoichiro

[1]Environmental Research Department,Technology Research Center, Taisei Corporation,Yokohama, JAPAN
[2]Technology Division, Taisei Corporation,Tokyo, JAPAN

ABSTRACT

In predicting the thermal environment of an indoor space affected seriously by the outdoor weather like an atrium using natural ventilation, it is essential to grasp the impact of the external outdoor weather precisely.

This report describes the result of the analysis on the outdoor and indoor regions including solar radiation analysis considering the date and hour, latitude and longitude taking the atrium under construction in Kyoto as an example.

The results are as follows.

(1) Simultaneous analysis of indoor and outdoor regions enables to review the indoor thermal environment in detail.

(2) Conducting solar radiation analysis considering the date and hour, latitude and longitude realizes analyses taking solar insolation and distribution inside a space into account.

(3) Conducting the analysis by changing the external wind velocity into 4 stages in this case proves that the indoor environment possibly becomes inferior under the conditions other than the calm state.

KEYWORDS

Case studies, CFD, Large premises, Natural ventilation

1.INTRODUCTION

In predicting the thermal environment of an indoor space affected seriously by the outdoor weather like a large space or atrium for example, it is essential to grasp the impact of the external weather (wind and solar radiation) precisely. Especially in the case when natural ventilation is applied, the entering and leaving air velocity at the opening strongly affects the indoor airflow distribution, pressure, and temperature distribution.

In analyzing an indoor environment with an opening facing the outdoor, although a few studies conducted analysis of the domain containing the indoor and outdoor, (He et al. 1996; Hosooka et al. 1996; Suwa et al. 1996) the impact of external wind is usually given as a boundary condition by assuming the entering wind through the opening by using the weather data conventionally. To reflect the impact of the external wind on the analysis precisely, however, it is necessary to conduct the analysis by reproducing the outdoor building. Regarding the solar radiation, the uniform heat generation onto floor surface is assumed conventionally, as the verification of the solar radiation and distribution inside the space with complicated configuration is difficult. However, as the heat generation distribution of solar radiation affects the temperature distribution and pressure distribution, the consideration of this heat generation distribution is more important particularly in the case of natural ventilation.

This report describes the result of the analysis on the outdoor and indoor regions taking the atrium under construction in Kyoto as an example. The building analyzed will be completed in August 1998, and the simulation accuracy will be verified after measurement.

2.OUTLINE OF ANALYSIS

2.1 Objective building

The objective building is an atrium under construction in Kameoka-City, Kyoto. The length of the atrium counts for about 210m, the maximum width about 25m and the height 20m. The glass area covering about 8,300m^2 locates at the top light section on the side wall. Ventilation is performed through the grilles installed at the east and west ends. At both side light sections of the atrium, 96 sets of ventilation fan with a capacity of 1,000m^3/h are installed. In addition, a pole type cooling unit (supply air

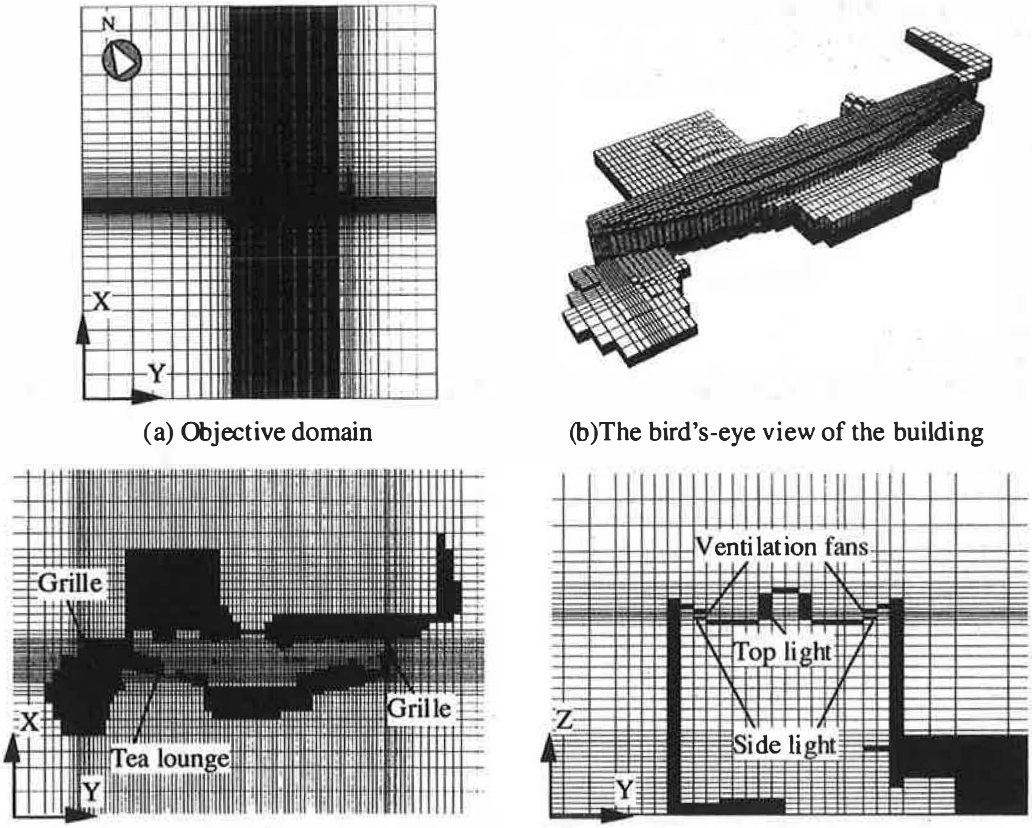

(a) Objective domain

(b)The bird's-eye view of the building

(c) Atrium X-Y cross section (FL+1.0m)

(d) Atrium Y-Z cross section at tea lounge

FIgure 1 Analysis model

Table 1 Outdoor temperature/humidity of Kameoka-City

	Outdoor temperature (°C)			Outdoor humidity (%)		
	Average	Lowest	Highest	Average	Lowest	Highest
1995. 9	22.7	15.3	29.3	62	31	93
10	17.3	6.6	26.4	79	33	98
11	8.4	2.0	16.1	69	31	98
12	3.8	-1.0	10.6	76	41	98
1996.1	3.1	-2.9	11.0	74	40	99
2	1.8	-4.5	14.3	74	34	99
3	6.2	-1.4	17.6	69	30	99
4	10.4	0.2	25.6	55	20	98
5	18.2	9.6	27.5	57	18	96
6	23.1	15.1	29.6	69	15	99
7	27.5	19.7	35.1	90	26	96
8	28.2	20.9	36.2	57	28	99

temperature 25 °C, supply air velocity 2.7m/s, supply airflow rate 1,200m^3/h) is installed at 4 spots in a part on the tea lounge of the atrium south side.

2.2 Analysis model

Figurel shows analysis model. The mesh partition counts for 118 in the X-direction, 67 in the Y-direction, and 50 in the Z-direction, 395,300 in total. Since natural ventilation is adapted inside the atrium of the objective building, the domain for calculation was defined as 750m in the atrium longer side direction (X axis), 800m in the atrium shorter side direction (Y axis), and 150m for the height (Z axis), including the surrounding of the building.

2.3 Weather condition

For weather data, that measured at a point about 500m from the southeast of the atrium in August, 1996 was used. Tablel shows the annual temperature/humidity data of Kameoka-City, Kyoto. Figure 2 shows the wind rose at 14:00 in August. Figure 3 shows the wind velocity frequency distribution at 14:00 (Z=18.0m). In the analysis, the 31.6°C representing the mean highest temperature was adapted. For the wind direction, the west-northwest representing the highest frequency value was adapted. For the wind velocity in the analysis was reviewed for that at a calm, 20% and 80% excess frequency wind velocity, and the maximum wind velocity. The wind velocity at the opening height was assumed by using 1/4 power multiplication law, as the measured height of the wind velocity counted for 43m.

2.4 Analyisis of solar radiation

Table2 shows the outline of solar radiation analysis. For the analysis of solar radiation was used a program (Urano et al. 1993) in which Radiocity method was adopted to predict three-dimentional distributions of solar radiation (Cohen et al. 1988). In analyzing solar radiation, the solar azimuth information was calculated from the building position and the date and hour, and the transmission amount of the glass surface with specified reflection ratio and transmission ratio against the direct solar radiation and sky solar radiation insolated into the analysis domain were calculated. Further, by analyzing the wall surface reflection of the light insolated into the building, the amount of light absorbed into each wall surface to use for thermal analysis. Table 3 shows the condition of analysis. Table 4 shows the physical value of each

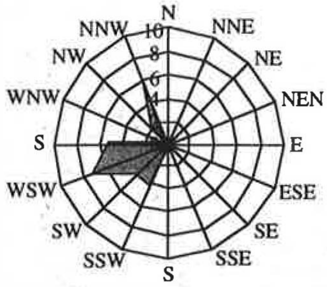

Figuire 2 Wind rose (14:00 August 1996)

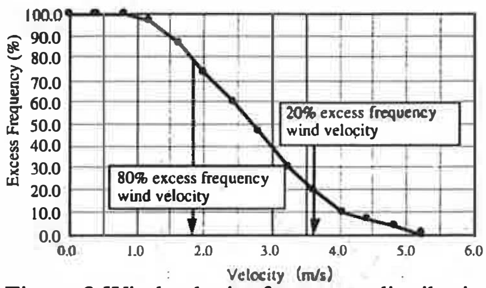

Figure 3 Wind velocity frequency distribution (Z=18.0m)(August 14:00 1996)

material additionally.

2.5 Thermal analysis

2.5.1 Basic equations

Table 5 shows the basic equations used for the analysis. Standard two-equation model of turbulence (Launder and Spalding 1972) was used and SIMPLE method (Patankar 1980) was adopted in this analysis.

2.5.2 Boundary condition

Vertical distribution of the wind velocity on the inflow boundaries was assumed by using 1/4 power multiplication law. The conditions of the upper air and the other side boundaries are free-slip. The boundary conditions on the solid boundaries are logarithmic law. Table 6 shows the overall heat transfer coefficient of each component. In the side light section at both sides of the atrium ceiling, ventilation fans with a total capacity of 9600m^3/h are installed. The opening including the grilles at the atrium both ends counts for 23.8m^2 (opening ratio of 0.34). The human load was assumed as 0.1 person/m^2 (5.5W/m^2).

2.5.3 Analysis cases

Table 7 shows the cases of analysis together. Assuming that the wind direction is west-southwest, the analysis was conducted for 4 stages from the calm to the maximum wind velocity according to the frequency distribution of wind velocity in August (Case1~4). Note that these analyses were

Table 2 Outline of solar radiation analysis

(1) Direct solar radiation

a) Clear sky

I_{ND}=Aexp(-B/sinh) (1)

I_{DH}=I_{DN}sinh (2)

I_{DNC}=I_{DN}(10.0-C)/10.0 (3)

b) Intermediate sky & overcast sky

where

I_{DN}=intensity of direct solar radiation incident upon a normal surface

I_{DH}=intensity of direct solar radiation incident upon a horizontal surface

A = virtual solar constant by month (Table A)

B = virtual consumption constant by month (Table A)

h = solar altitude

C = cloud amount (= 0.0 for clear sky; =10.0 for overcast sky; = others for intermediate sky)

Table A (ASHRAE 1997)

Month	A (W / m²)	B	C
1	1230	0.142	0.058
2	1215	0.144	0.060
3	1186	0.156	0.071
4	1136	0.180	0.097
5	1104	0.196	0.121
6	1088	0.205	0.134
7	1085	0.207	0.136
8	1107	0.201	0.122
9	1151	0.177	0.092
10	1192	0.160	0.073
11	1221	0.149	0.063
12	1233	0.142	0.057

(2) Diffuse sky solar radiation

a) Clear sky

I_{SKY}=I_{DN}•C (Table A) (4)

b) Intermediate sky & overcast sky

I_{SKY}=I_{TH}(1.0+0.015C-0.009C^2) - I_{DNC} (5)

where

I_{SKY}=intensity of diffuse sky solar radiation r radiation incident upon a horizontal surface in clear sky

I_{TH}=intensity of total solar radiation incident upon a horizontal surface (=I_{DN}+ I_{SKY})

C = cloud amount (0.0 to 10.0)

The intensity of diffuse sky solar radiation is obtained in the following manner. A hemisphere with a radius large enough to neglect the spatial scale of an analysis domain is assumed virtually to be sky.

The hemisphere is divided into 151 (Tregenza 1987) elements, and the intensity of diffuse sky solar radiation is divided and set to each section. The shape factor of sky is taken into account by judging obstacles between an element and plane element, and the intensity of diffuse sky solar radiation is obtained. Relative luminance, L_{rcl}, on the hemisphere, n is given by the following equation.

$$L_{rcl}(Z_s, Z, \zeta) = \frac{f(\zeta)\cdot\phi(Z)}{f(Z_s)\cdot\phi(0^\circ)} = L_{rcl}[n] \quad (6)$$

where

ζ = angular distance between a sky element and the sun

Z = zenith distance of a sky element (π/2-γ, : γ = latitude of a sky element)

Z_s= zenith distance of the sun (π/2-h, : h= latitude of the sun)

$f(\zeta) = 0.91+10\cdot\exp(-3\zeta)+0.45\cos^2\zeta$ (7)

$\phi(Z) = 1 - \exp(-0.32\cdot\sec Z)$ (8)

The angular distance between a sky element and the sun, x in given by the following equation.

$$\cos\zeta = \sinh\sin\gamma + \cosh\cdot\cos\gamma\cdot\cos(|\bar{\alpha}_s\cdot\bar{\alpha}|) \quad (9)$$

where

α_s= azimuth vector on the sun

α = azimuth vector of a sky element

The sum of relative luminance, R_{sd}, is expressed as ,

$$R_{rcl} = \sum_{n=1}^{151} L_{rcl}[n] \quad (10)$$

Therefore, the intensity of diffuse sky solar radiation, $I_{SKY}[n]$, on the hemisphere, n is given as follows.

$I_{SKY}[n] = I_{SKY}\cdot L_{rcl}[n]/R_{rcl}$ (11)

(Relative luminance distribution equation in CIE standard's clear sky, intermediate sky, and overcast sky: cloud amount; = 0.0 for clear sky; =10.0 for overcast sky; = others for intermediate sky)

(3) Reflected solar radiation

Radiocity method is adopted. The method allows reduction in computational volume within a given accuracy as well as to deal with complex shapes.

*Projection angle, number of projections divided, number of objects divided, and short wave computational limitations are input values.

*Short wave reflectivity and transmittance are default values (and can be inputted for each material.)

Table 3 Condition of solar radiation analysis

Time:June 21 14:00 (Solstitial point)

Latitude,Longitude : 35.167, 135.73 (Kyoto)

Cloudiness,Cloud ceiling height : 0.0, 0.8 (Fine weather, Upper clouds)

Table 4 Physical values of each material

Section	Material	Solar radiation rate (%)		
		Reflection	Transmission	Absorption
North side external wall glass	Clear glass (t=15mm)	7	64	19
South side external wall glass	Heat reflection glass (t=15mm)	18	49	23
Building body	Concrete with bright color	40	0	60
1F floor	Red brick	45	0	55
Other sections than top light, sidelight and roof of sidelight	Roof(Polyvinyl chloride sheet + Roof board) +Ceiling (Air layer + Plaster board + Non-combustible rock wool)	60	0	40
Roof of sidelight	Galvanized steel plate	20	0	80
Top light and side lightt	Wired transparent glass (t=10mm)	7	70	23

Table 5 Basic equations for the analysis

$$\frac{\partial u_j}{\partial x_j} = 0 \quad (12)$$ Continuity equation

$$\frac{\partial u_j}{\partial t} + \frac{\partial u_j u_i}{\partial x_j} = -\frac{1}{r}\frac{\partial P}{\partial x_j} + v\frac{\partial^2 u_j}{\partial x_j \partial x_j} + f_i - g_i \beta (T - Tref) \quad (13)$$ Momentum equation

$$\frac{\partial_r C_p T}{\partial t} + \frac{\partial u_j r C_p T}{\partial x_j} = \frac{\partial}{\partial x_j} K \frac{\partial T}{\partial x_j} + q \quad (14)$$ Energy equation

$$\frac{\partial k}{\partial t} + \frac{\partial u_j k}{\partial x_j} = \frac{\partial}{\partial x_j}\left(\frac{\nu_t}{\sigma_\varepsilon}\frac{\partial k}{\partial x_j}\right) + G_s + G_T - \varepsilon \quad (15)$$ Transport equation for turbulent kinetic energy

$$\frac{\partial \varepsilon}{\partial t} + \frac{\partial u_j \varepsilon}{\partial x_j} = \frac{\partial}{\partial x_j}\left(\frac{\nu_t}{\sigma_\varepsilon}\frac{\partial \varepsilon}{\partial x_j}\right) + C_1 \frac{\varepsilon}{k}(G_s + G_T)(1 + C_3 R_f) - C_2 \frac{\varepsilon^2}{k} \quad (16)$$ Transport equation for dissipation rate

$$G_s = \nu_t\left(\frac{\partial u_i}{\partial x_j} + \frac{\partial u_j}{\partial x_i}\right)\frac{\partial u_i}{\partial x_j} \quad (17), \quad G_T = g_i \beta \frac{\nu_t}{\sigma_t}\frac{\partial T}{\partial x_i} \quad (18), \quad R_f = -\frac{G_T}{G_s + G_T} \quad (19)$$

$\sigma_k = 1.0$, $\sigma_\varepsilon = 1.3$, $C_1 = 1.44$, $C_2 = 1.92$, $C_3 = 0.0$, $C_4 = 0.09$ Turbulence model constants

x_j	: space coordinate	g_i	: gravitational acceleration
u_j	: velocity	ß	: thermal expansion coefficient
t	: time	T	: temperature
ρ	: air density	T_{ref}	: reference temperature
P	: pressure	k	: turbulence energy
ν_t	: eddy kinematic viscosity	ε	: dissipation rate

Table 6 Overall heat transfer coefficient

Section	Overa l heat transfer coefficient ($W/m^2 {}^\circ C$)
Top light :wired transparent glass (t=10mm)	5.60
Roof of side light	3.94
North side externa wall glass (t=15mm)	5.40
South side externa wall glass (t=15mm)	5.40
Roof + Ceiling	1.20

Table 7 Ana ysis cases

	External wind	Mechanical ventilation	Spot cooling	Door opening
Case 1	Calm	off	off	close
Case 2	80% excess frequency wind velocity	off	off	close
Case 3	20% excess frequency wind velocity	off	off	close
Case 4	Maximum wind velocity	off	off	close
Case 5	80% excess frequency wind velocity	on	off	close
Case 6	80% excess frequency wind velocity	on	on	open

conducted without applying mechanical ventilation and spot cooling. The analyses were also conducted with only mechanical ventilation applied (Case 5), and with both mechanical ventilation and spot cooling applied while opening all doors facing the atrium about $50m^2$ (Case 6).

3.RESULT OF ANALYSES

3.1 Analysis of solar radiation

Figure 4 shows the result of the solar radiation analysis (plan). In the domain covered fully with glass from the floor of the atrium south surface extremely affected by

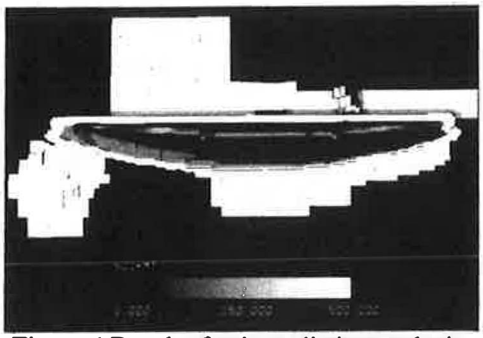

Figure 4 Result of solar radiation analysis (Floor surface)(unit:w/m^2)

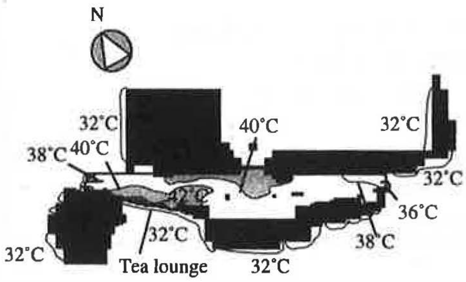

(a) Calm

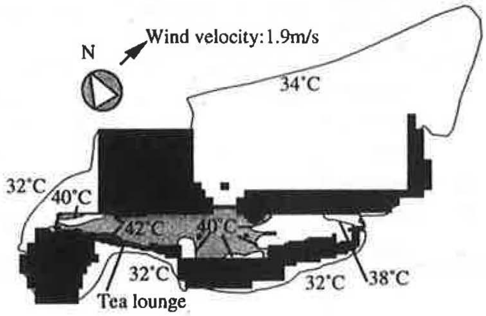

(b) 80% excess frequency wind velocity

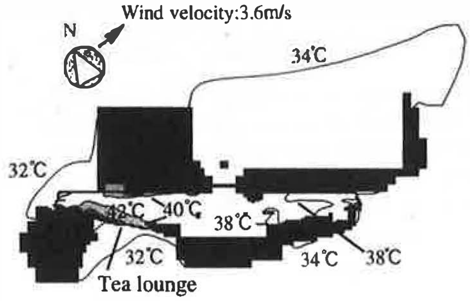

(c) 20% excess frequency wind velocity

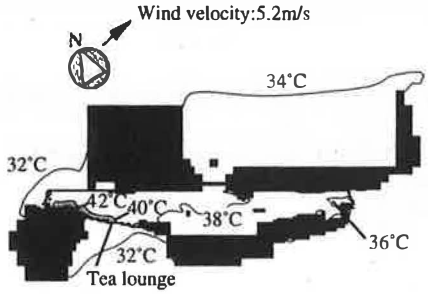

(d)Maximum wind velocity

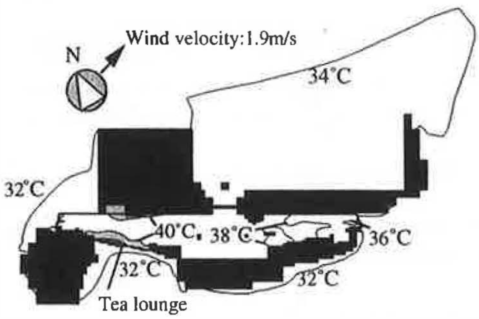

(e) Mechanical ventilation

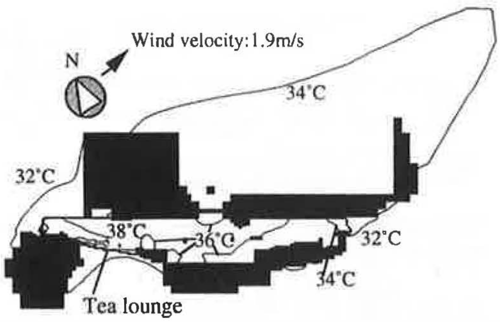

(f) Mechanical ventilation,spot cooling and door opning

Figure 5 Result of thermal analysis (FL+3.5m) solar radiation to the ceiling, the heating amount counts for 200W/m^2 approximately. The average heating amount of the total floor area of the atrium counts for 47W/m^2 approximately. Using the above analysis result, the thermal analysis was conducted.

3.2 Thermal Analysis

Figure 5 shows the result of the thermal analysis conducted at FL + 3.5m. The temperature inside the atrium is high around the tea lounge as a whole allowing the existence of about 42 °C When the cases from 1 to 4 are compared, the worst state does not appear at the calm but at 80% excess frequency wind velocity. The wind flow entered from the east side moves over a distance mostly doubling that of movement by the wind entered from the west side. Regarding the wind flow volume entering the atrium, that from the west side grille decreases while that from the east grille increases as the wind velocity increases. For this reason, even the region near the west grille is covered by the wind flow from the east grille thus increasing the temperature around the tea lounge.

From the analyses results of Cases 1 ~ 4, it can be understood that the region with extremely high temperature can be existed in the atrium if only natural ventilation is adapted. Even with ventilation fans operated, the temperature shows about 38 °C as a whole, and about 42°C near the tea lounge. When a pole type cooling equipment are installed at 4 spots in a part of the region of atrium south side, and the doors facing the atrium are opened about 50m^2 (Case 6), the temperature shows about 36 °C as a whole, and less than 40 °C around the tea lounge where higher temperature exists in other cases.

4.CONCLUSION

This report describes our analyses conducted for the analysis domain containing the indoor and outdoor of a building taking the atrium under construction in Kyoto as an example. As a result, the following views are obtained.

(1) Simultaneous analysis of indoor and outdoor regions enables to review the indoor thermal environment in detail.

(2) In analysis, it is important to select the wind direction and wind velocity based on the statistical data of the wind direction and wind velocity of a construction site.

(3) Conducting solar radiation analysis considering the date and hour, latitude and longitude realizes analysis taking solar insolation and distribution inside a space into account.

(4) Conducting the analysis by changing the external wind velocity into 4 stages in this case proves that the indoor environment possibly becomes inferior under the conditions other than the calm state.

(5)Mechanical ventilation, spot cooling and door opening adapted at an outdoor temperature of 31.6 °C allows the temperature in the most region of the atrium to be about 36 °C.

The building taken as an analysis example will be completed in August 1998. We will verify the simulation accuracy after measurement.

The analysis this time was conducted by assuming the highest temperature in August and fine weather condition. However it is unknown how is the frequency when such the state appear in a year. This will be our future problem. The impact of heat storage by building body will also be our future problem.

ACKNOWLEDGEMENTS

The authors wish to express their thanks to Mr. Uichi Inouye and Mr. Shoji Goto, UICHI INOUYE RESEARCH INSTITUTE, Mr. Hideki Yamaguchi, YOSHIRO IKEHARA ARCHITECT & ASSOCIATES, Mr. Takeshi Sambe, SAKURAI SYSTEM Co.,Ltd. and Mr. Kenji Yokoyama, DAIICHI KOGYO Co.,Ltd. for their cooperation in conducting this analysis.

REFERENCES

ASHRAE (1997) *1997 ASHRAE handbook-fundamentals*. American Society of Heating, Refrigerating and Air-Conditioning Engineers, Inc. Atlanta.

Cohen, M. F. ,Chen, S. E., Wallace, J. R. and Greenberg, D. P. (1988) A progressive refinement approach to fast radiocity image generation. *Computer Graphics*, 22 , 75-84

He, P., Katayama, T., Hayashi, T., Tsutsumi, J., Tanimoto, J., Hosooka, I., (1996), Examination of the effects of wall thickness and bay windows on cross-ventilation by CFD, *Proceedings ROOMVENT'96*. Yokohama, Japan.

Hosooka, I., Katayama, T., Hayashi, T., Tsutsumi, J., Tanimoto, J., He, P., (1996) Examination of the influence of enclosing fences on cross-ventilation through a house by CFD, *Proceedings ROOMVENT'96*. Yokohama, Japan.

Launder, B. E. and Spalding, D. B. (1972) *Mathematical models of turbulence.* Academic Press.

Patankar, S. V. (1980) *Numerical heat transfer and fluid flow.* Hemisphere Publishing Corp. New York.

Suwa, Y., Omote, Y., Honma, Y., Otaka, K., Hashimoto, N., (1996) A study on the characteristics of air ventilation and thermal condition in a large indoor space with opening, *J. Archit. plann. Environ. Eng., Architectural Institute of Japan*, No.481,51-60.

Tregenza, P. R. (1987) Subdivision of the sky hemisphere for luminance measurements. *Lighting Res. Tech.*, 19,13-14.

Urano, A., Morikawa, Y., Saito, M. and Terasaka, T. (1993) Engineering approaches to predicting urban thermal environment (Part2) Numerical simulation of radiation environment. *Taisei Technical Research Report.*, 26, 339-344